



Observation of $K^+ \rightarrow \pi^+ \pi^0 \pi^0 \gamma$ decay

A. V. Artamonov¹, V. N. Bychkov³, S. V. Donskov¹, A. P. Filin¹, S. N. Filippov², A. M. Gorin¹, E. N. Gushchin², A. V. Inyakin¹, G. D. Kekelidze³, G. V. Khaustov¹, S. A. Kholodenko^{1,b}, A. A. Khudiyakov², V. N. Kolosov¹, V. I. Kravtsov², Yu. G. Kudenko^{2,c}, A. V. Kulik^{2,a}, V. F. Kurshetsov¹, V. A. Lishin¹, V. M. Lysan³, M. V. Medynsky¹, V. F. Obratsov¹, A. V. Okhotnikov¹, V. A. Polyakov¹, A. Yu. Polyarush², V. I. Romanovsky¹, V. I. Rykalin¹, A. S. Sadovsky¹, V. D. Samoylenko¹, M. M. Shapkin¹, I. S. Tiurin¹, V. A. Uvarov¹, O. P. Yushchenko¹, B. Zh. Zalikhanov³

¹ NRC "Kurchatov Institute"-IHEP, 142281 Protvino, Russia

² Institute for Nuclear Research, Russian Academy of Science, 117312 Moscow, Russia

³ Joint Institute of Nuclear Research, 141980 Dubna, Russia

Received: 31 October 2023 / Accepted: 13 March 2024 / Published online: 2 April 2024

© The Author(s) 2024

Abstract The $K^+ \rightarrow \pi^+ \pi^0 \pi^0 \gamma$ decay is observed by the OKA collaboration. About 60 events of the decay observed with signal:noise ≈ 1 . The branching ratio obtained by normalization to $K^+ \rightarrow \pi^+ \pi^0 \pi^0$ is measured to be $(3.7 \pm 0.9(stat) \pm 0.3(syst)) \times 10^{-6}$ for $E_\gamma^* > 10$ MeV. The branching ratio, γ energy spectrum and angular distribution are consistent with ChPT prediction.

1 Introduction

The present experimental status of the $K \rightarrow \pi^+ \pi^0 \pi^0 \gamma$ decays is rather meager [1]. So far the observation is claimed by the single experiment [2] with statistics of 5 events and $BR = (7.6_{-3.0}^{+6.0}) \times 10^{-6}$. The radiative photon is generated predominantly via internal bremsstrahlung with infrared pole at $E_\gamma = 0$. Compared to the study of $K^+ \rightarrow \pi^+ \pi^+ \pi^- \gamma$ decay reported by us earlier [3] the $K^+ \rightarrow \pi^+ \pi^0 \pi^0 \gamma$ decay has less charged particles in the final state, i.e the bremsstrahlung component is less pronounced and there is a chance to detect more interesting effects. In this article we present the observation and measurement of that decay with considerably improved precision. This decay has certain interest for the theory, in par-

ticular, for the chiral perturbation theory (ChPT). The calculations in the next-to-leading order in this framework are done in [1,4] predicting the branching ratio at 3.76×10^{-6} for $E_\gamma^* > 10$ MeV. It is interesting to compare this result to the experimental data.

2 The OKA setup

The OKA is a fixed target experiment dedicated to the study of kaon decays using the decay in flight technique. It is located at NRC "Kurchatov Institute"-IHEP in Protvino (Russia). A secondary kaon-enriched hadron beam is obtained by an RF separation with the Panofsky scheme. The beam is optimized for the momentum of 17.7 GeV/c with kaon content of about 12.5% and intensity up to 5×10^5 kaons per U-70 accelerator spill.

The OKA setup (Fig. 1) makes use of two magnetic spectrometers along with an 11 m long decay volume (DV) filled with helium at atmospheric pressure and equipped with a guard system (GS) of lead-scintillator sandwiches mounted in 11 rings inside the (DV) for photon veto. It is complemented by an electromagnetic calorimeter BGD [5] with a wide central opening.

The first magnetic spectrometer measures momentum of the beam particles with a resolution of $\sigma_p/p \sim 0.8\%$. It consists of a vertically (y) deflecting magnet M_1 surrounded by a set of 1 mm pitch (beam) proportional chambers $BPC_{(1Y, 2Y, 2X, \dots, 4Y)}$. It is supplemented by two threshold Cherenkov

^a e-mail: alex.kulik@gmail.com (corresponding author)

^b Also at INFN, Sezione di Pisa, 3-56127 Pisa, Italy

^c Also at Moscow Institute of Physics and Technology (MIPT), and National Research Nuclear University (MEPhI), Moscow, Russia

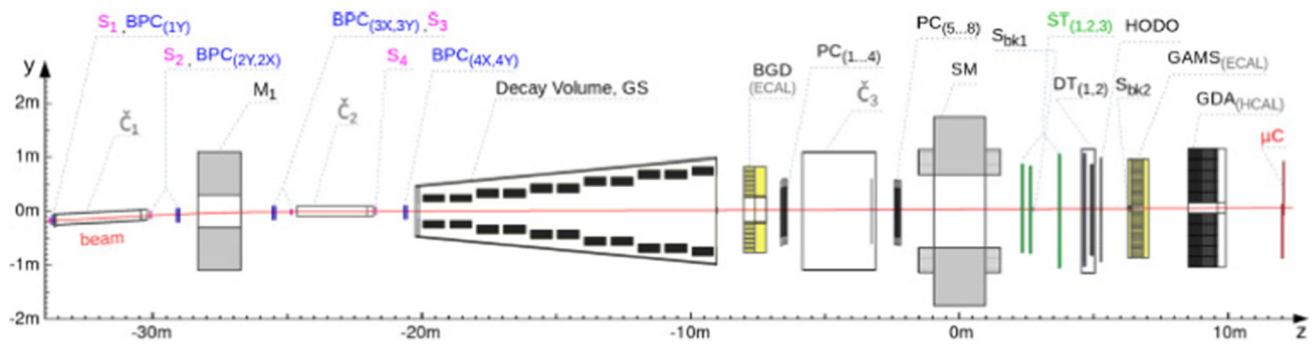


Fig. 1 Schematic elevation view of the OKA setup. S_{1-4} – beam scintillation counters; $C_{1,2}$ – gas Cherenkov counters; BPC_{1-4} – beam proportional chambers; M_1 – beam analyzing magnet; GS – guard system; PC_{1-8} – proportional chambers for secondary track; SM – secondary

track analyzing magnet; ST – straw tubes; DT – drift tubes; HODO – matrix hodoscope; S_{bk1}, S_{bk2} – beam killer counters; BGD, GAMS – electromagnetic calorimeters; GDA – hadron calorimeter; μC – muon counter. See the text for details

counters \check{C}_1, \check{C}_2 for kaon identification and by beam trigger scintillation counters $S_{(1)}, S_{(2)}, S_{(4)}$. To measure the charged tracks from decay products the second magnetic spectrometer is used (with resolution of $\sigma_p/p \sim 1.3-2\%$ for momentum range of 2–14 GeV/c). It consists of a wide aperture $200 \times 140 \text{ cm}^2$ horizontally (x) deflecting magnet SM with $\int Bdl \sim 1 \text{ Tm}$ surrounded by tracking stations: proportional chambers $PC_{(1,\dots,8)}$, straw tubes $ST_{(1,2,3)}$ and drift tubes $DT_{(1,2)}$. A matrix hodoscope HODO is used to improve time resolution and to link x – y projections of a track.

At the end of the setup there are: an electromagnetic calorimeter $GAMS_{(ECAL)}$ of $15X_0$ (consisting of ~ 2300 $3.8 \times 3.8 \times 45 \text{ cm}^3$ lead glass blocks) [6] with the energy resolution of $\sigma_E/E = 0.015 + 0.1/\sqrt{E}$ and the space resolution of 2–8 mm, a hadron calorimeter $GDA_{(HCAL)}$ of 5λ (constructed from 120 $20 \times 20 \text{ cm}^2$ iron-scintillator sandwiches with WLS plates readout) and a wall of $4 \times 1 \text{ m}^2$ muon counters μC behind the hadron calorimeter.

More details on the OKA setup can be found in [7, 8].

3 The data and the analysis procedure

Two sequential runs of data with beam momentum of 17.7 GeV/c recorded by OKA collaboration in 2012 and in 2013 are analysed in search for $K^+ \rightarrow \pi^+\pi^0\pi^0\gamma$ decay.

The main trigger requires a coincidence of 4 beam scintillation counters, a combination of two Cherenkov's (\check{C}_1 sees pions, \check{C}_2 pions and kaons) and, finally, anticoincidence of two scintillation counters S_{bk1}, S_{bk2} , located on the beam axis after the magnet to suppress undecayed beam particles: $\text{Tr}_{K\text{decay}} = S_1 \cdot S_2 \cdot S_3 \cdot S_4 \cdot \bar{C}_1 \cdot \bar{C}_2 \cdot \bar{S}_{bk}$. The trigger additionally requires an energy deposition in GAMS-2000 e.m. calorimeter higher than 2.5 GeV to suppress the dominating $K^+ \rightarrow \mu^+\nu$ decay: $\text{Tr}_{GAMS} = \text{Tr}_{K\text{decay}} \cdot (E_{GAMS} > 2.5 \text{ GeV})$.

The Monte Carlo (MC) statistics is generated with Geant-3.21 [9] program comprising a realistic description of the setup. The MC events are passed through full OKA reconstruction procedures.

For the estimation of the background to the selected data set, a sample of the Monte Carlo events with six main decay channels of charged kaon ($\pi^+\pi^0, \pi^+\pi^0\pi^0, \pi^+\pi^0\gamma, \mu^+\nu\gamma, \pi^0\mu^+\nu, \pi^0e^+\nu$) mixed accordingly to their branching fractions, with the total statistics ~ 10 times larger than that of the recorded data sample is used. Every MC event has a weight $w \sim |M|^2$ where M is the matrix element of the decay. The weights for the 3-body decays are calculated from the data, presented in PDG [10], the matrix element of the $K^+ \rightarrow \pi^+\pi^0\pi^0\gamma$ decay comes from [4]. The pileup and processes when the beam kaon scatters or interacts while passing the setup are also added.

3.1 Event selection

The total of $\sim 3.6 \times 10^9$ events with kaon decays are logged in of which $\sim 8 \times 10^8$ events are reconstructed with a single charged particle in the final state. The primary selection criteria are:

- The secondary positive track is neither e^+ (by E/p ratio) nor μ^+ (no signal in μC counter).
- The angle between the beam and the secondary track $\Theta > 2 \text{ mrad}$ (to suppress the beam background); the distance between the beam and secondary track $< 1 \text{ cm}$.
- The decay vertex is within the decay volume.
- Only one segment of the charged track downstream the analysing magnet.
- 5 γ with energy $E > 0.5 \text{ GeV}$ detected.
- Out of all possible combinations of 4 γ s the one with minimal value of $R^2 = (m_{ij} - m_{\pi^0})^2 + (m_{kl} - m_{\pi^0})^2$, $ij \neq$

kl is identified as $\pi^0\pi^0$ and the remaining 5th, “stray” γ considered bremsstrahlung.

- 5th γ hits GAMS rather than BGD.
- At least one out of 4 γ , making $\pi^0\pi^0$, hits GAMS. This has some influence since GAMS is in trigger and BGD is not.
- 5th γ energy in K^+ rest frame is $10 < E_\gamma^*(measured) < 50$ MeV.

About 230k events selected at this stage. Per MC simulation the only background process surviving this selection is non-radiative decay $K^+ \rightarrow \pi^+\pi^0\pi^0$ of similar topology less one γ . The extra “ghost” γ easily emerges due to the fluctuations of π^+ hadronic shower in GAMS e.m. cal. This background decay is ≈ 5000 times more frequent (1.76%) than the radiative decay in question thus presenting a major challenge in this analysis. We employ a Radial Basis Function Network (RBFN) neural net [11] to suppress this background. MC events of $K^+ \rightarrow \pi^+\pi^0\pi^0$ and $K^+ \rightarrow \pi^+\pi^0\pi^0\gamma$ decays passed the primary selection criteria are used to train the neural network (NN); the training set contains 100k events of each type. For the inputs to the NN we use the variables relevant to discrimination between two types of events:

- $\Delta E = E_{\pi^+} + \sum_{i=1}^5 E_{\gamma_i} - E_{beam}$ - the energy balance in the event. Any extra γ piled up on top of major background process $K^+ \rightarrow \pi^+\pi^0\pi^0$ results in $\Delta E > 0$.
- E_γ - the 5th γ energy.
- d_γ - distance from the 5th γ to the track at GAMS plane.
- $\chi_\gamma^2 - \chi^2$ of the 5th γ shower shape fit. All 3 bullets above may help discriminating the events where the fluctuations of π^+ shower in GAMS may mimic an extra γ .
- $\chi_{\pi^+\pi^0\pi^0}^2 - \chi^2$ of 3C-fit to $\pi^+\pi^0\pi^0$. Good χ^2 is likely to come from $\pi^+\pi^0\pi^0$.
- $\chi_{\pi^+\pi^0\pi^0\gamma}^2 - \chi^2$ of 3C-fit to $\pi^+\pi^0\pi^0\gamma$. Bad χ^2 suggests something wrong with the event.
- $M_{\pi^+\pi^0\pi^0} - \text{mass of } \pi^+\pi^0\pi^0 \text{ in 3C-fit. } \pi^+\pi^0\pi^0\gamma\text{-event fitted to } \pi^+\pi^0\pi^0\text{-hypothesis results in the mass shifted to the lower values due to disregarded } \gamma. \text{ (In 3C fit the } \gamma \text{ energies are fitted under 3 kinematic constraints: } m_{\gamma_1\gamma_2} = m_{\gamma_3\gamma_4} = m_{\pi^0} \text{ and the total energy of the secondaries equals to the beam energy.)}$

On its output the RBFN produces a real number. Moving the output threshold offers control over signal:background ratio (Fig. 2).

The sample of 230k events left after primary selection is processed by this neural net to obtain the mass spectra in Fig. 3. The mass is calculated per

$$m^2 = E^2 - \vec{p}^2;$$

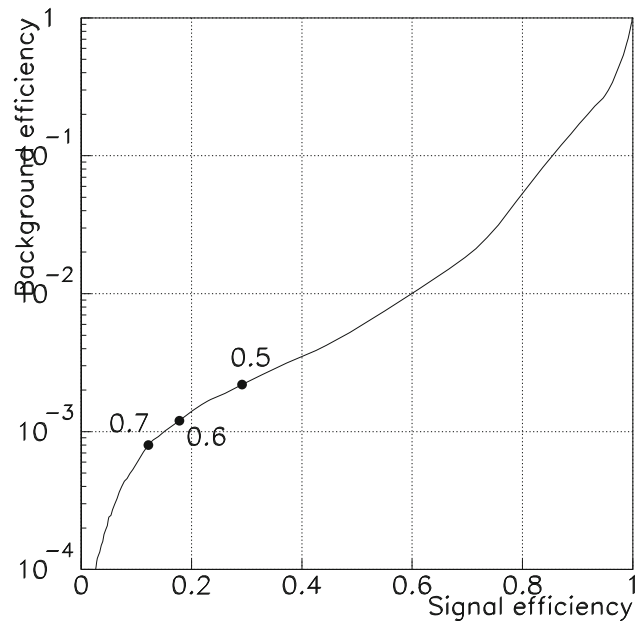


Fig. 2 Neural net performance, the axes are normalized to the MC sample used for training. With the thresholds used in this analysis (shown with bullets) the NN can suppress the background 1000 times while retaining about 1/4 of good events

$$E = \sqrt{p_{\pi^+}^2 + m_{\pi^+}^2} + E_{\pi_1^0} + E_{\pi_2^0} + E_\gamma, \quad \vec{p} = \vec{p}_{\pi^+} + \vec{p}_{\pi_1^0} + \vec{p}_{\pi_2^0} + \vec{p}_\gamma \quad (1)$$

where E_i, \vec{p}_i, m_i stand for the energies, momenta and mass of the particles in the final state. Clear peak is seen in the mass spectra for 3 different thresholds on RBFN output. The observed peak width is dominated by the GAMS energy resolution and is reproduced by MC.

3.2 Fitting mass spectra

The mass spectra in Fig. 3 are fitted in order to determine the number of events of the decay. We tried two different background shape models:

- MC shape:

$$Data = \alpha \times MC(K^+ \rightarrow \pi^+\pi^0\pi^0\gamma) + \beta \times MC(K^+ \rightarrow \pi^+\pi^0\pi^0) \quad (2)$$

with free scaling parameters α, β ;

- Gaussian shape + second order polynomial, peak position and width being free parameters.

The numbers for different fits came out close within errors (Table 1). We adopt the fit with MC background shape and $RBFN > 0.5$ as the basis to obtain the BR because in this case the background shape is more smooth due to better MC

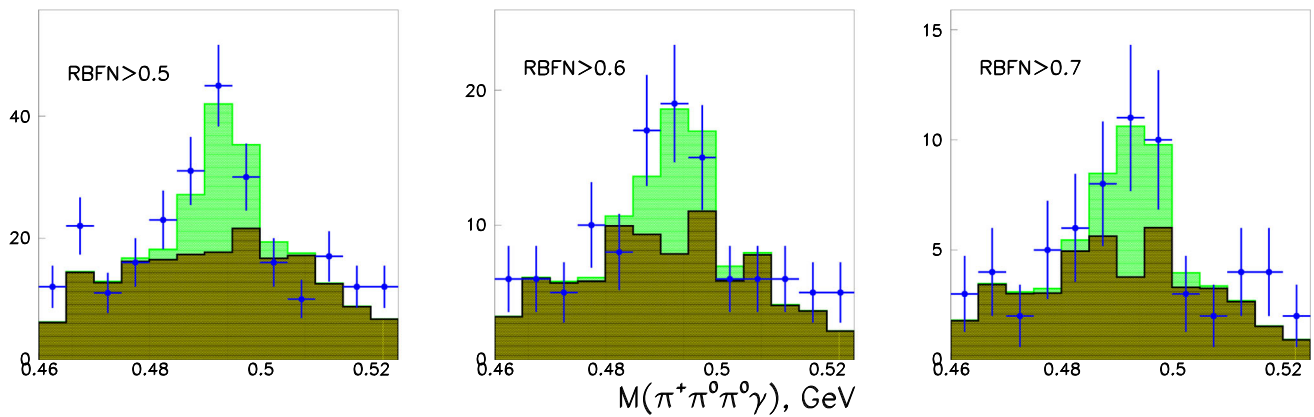


Fig. 3 Mass spectra for different cuts on RBFN output; data are the points with error bars, the MC background and signal are the dark and light histograms respectively

Table 1 Number of $K^+ \rightarrow \pi^+\pi^0\pi^0\gamma$ events in the peak and corresponding branching ratios in units of 10^{-6} for different RBFN thresholds and background models

RBFN >	MC	G+P2
0.5	53.8 ± 13	63 ± 14.2
χ^2/N_{DF}	15.3/10	7.5/6
BR, 10^{-6}	3.73 ± 0.9	4.37 ± 0.98
0.6	23.5 ± 8.9	30.7 ± 9
χ^2/N_{DF}	7.3/10	2/6
BR, 10^{-6}	2.73 ± 1.03	3.56 ± 1.04
0.7	15.2 ± 6.8	19.9 ± 7.5
χ^2/N_{DF}	6.3/10	4.9/6
BR, 10^{-6}	2.63 ± 1.18	3.44 ± 1.3

statistics thus the error is driven by limited data rather than the size of MC sample. Also the peak is more statistically significant in this case, the p-value for the fit to background hypothesis is $p = 9 \times 10^{-6}$. The other 5 fits are used to estimate possible systematic errors. In particular, the background shape in G+P2 fits do not rely on MC at all so the close numbers in columns 2 and 3 of Table 1 prove the result insensitive to the background shape model.

4 Branching ratio

The decay of similar topology, $K^+ \rightarrow \pi^+\pi^0\pi^0$, used for normalization to cancel out most of uncertainties in efficiency calculation. We have about 2×10^6 of those at hand with no considerable background (Fig. 4).

$$BR_{\pi^+\pi^0\pi^0\gamma} = \frac{n_{\pi^+\pi^0\pi^0\gamma}}{n_{\pi^+\pi^0\pi^0}} \times \frac{\varepsilon_{\pi^+\pi^0\pi^0}}{\varepsilon_{\pi^+\pi^0\pi^0\gamma}} \times BR_{\pi^+\pi^0\pi^0} \quad (3)$$

where \mathbf{n} , ε and \mathbf{BR} are the numbers of detected events, detection efficiencies and branching ratios. The detection efficiencies for both decays obtained through MC simulation. For $RBFN > 0.5$ $\varepsilon_{\pi^+\pi^0\pi^0\gamma} = 0.0205$, $\varepsilon_{\pi^+\pi^0\pi^0} = 0.141$. Due to the infrared pole in bremsstrahlung amplitude we quote the BR for the γ energy in K^+ rest frame $E_\gamma^* > 10$ MeV. The choice of 10 MeV cutoff is driven by our experimental setup being insensitive to lower energy γ s. There is a slight (~ 1 MeV) difference between the true and observed γ energies due to finite resolution. It is known from the simulation that the sample in Fig. 3, left is **not** contaminated with events with $E_\gamma^*(true) < 10$ MeV. Then by normalizing the detection efficiency $\varepsilon_{\pi^+\pi^0\pi^0\gamma}$ to the number of simulated events with $E_\gamma^*(true) > 10$ MeV we obtain the branching ratio not affected by the resolution on E_γ^* .

$$\begin{aligned} \frac{BR(K^+ \rightarrow \pi^+\pi^0\pi^0\gamma)}{BR(K^+ \rightarrow \pi^+\pi^0\pi^0)} &= (2.1 \pm 0.5) \times 10^{-4}; \\ BR(K^+ \rightarrow \pi^+\pi^0\pi^0\gamma) &= (3.7 \pm 0.9) \times 10^{-6}, \\ E_\gamma^* &> 10 \text{ MeV}. \end{aligned} \quad (4)$$

5 γ spectrum and angular distribution

The area around K^+ mass ($0.485 < m(\pi^+\pi^0\pi^0\gamma) < 0.505$) of the spectrum in the leftmost frame of Fig. 3 (RBFN>0.5) selected for this study. Scaled MC background γ spectrum was then subtracted from the γ spectrum of selected events:

$$\frac{dn}{dE_\gamma^*} = \left(\frac{dn}{dE_\gamma^*} \right)_{exp} - \beta \times \left(\frac{dn}{dE_\gamma^*} \right)_{bkgMC}, \quad (5)$$

with scaling factor β taken from the fit (2) of the $RBFN > 0.5$ mass spectrum. E_γ^* is the γ energy in K^+ rest frame. The distribution over the angle between γ and π^+ obtained in the

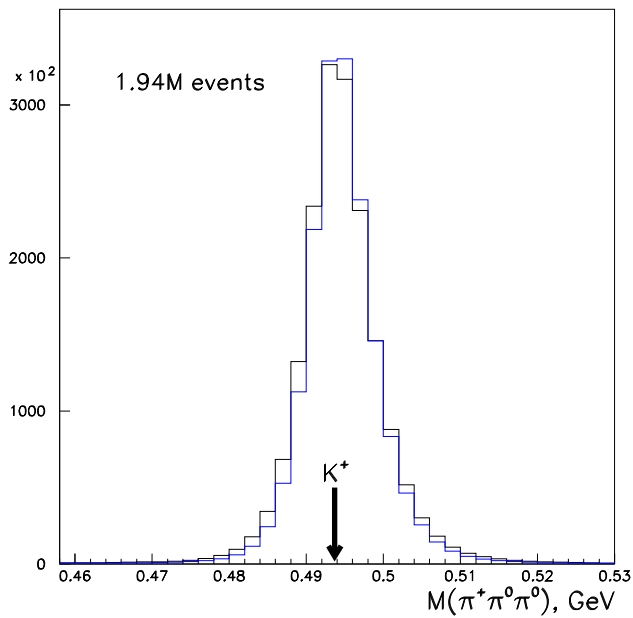


Fig. 4 Observation of $K^+ \rightarrow \pi^+\pi^0\pi^0$ decay used for normalization: data (black) and MC (blue)

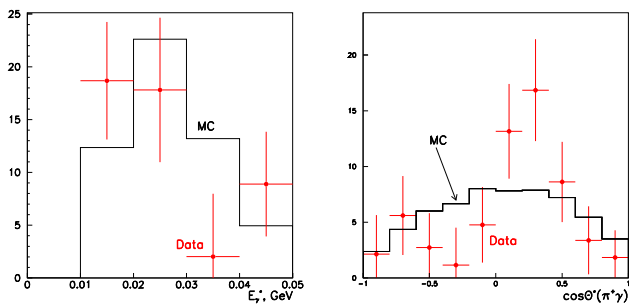


Fig. 5 Energy spectrum of γ and the angle between γ and π^+ in K^+ rest frame

same way. The resulting energy spectrum and angular distribution agree with ChPT prediction although the errors are large (Fig. 5). Both spectra are severely distorted by detection efficiency and complex selection criteria.

6 Systematic errors

The systematic errors in the measured BR are mostly cancel out because they are almost the same in the signal and normalization processes. That is the dominant contribution to the systematic error is due to the radiative photon measurement. The BR values derived from the mass spectra fits with different RBFN thresholds and background models mutually agree. Based on Table 1 we conclude that there are no systematics introduced by the fit beyond statistical errors. The MC estimate of the other sources comes out well below 25% statistical error:

- Wrong γ combination. Per MC the processing algorithm picks the wrong γ combination for $\pi^+\pi^0$ in 4.5% of events identified as $\pi^+\pi^0\pi^0\gamma$. In this case the mass peak broadens 3-fold contributing more to the background than to the peak.
- γ detection threshold varied from 0.4 to 0.6 GeV, 4% variation in BR.
- GAMS threshold curve. The triggering efficiency raises gradually from 0 to 1 with the GAMS energy deposition increase [12]. The MC study showed detection efficiencies for both decays being insensitive to particular shape of this curve down to 1%.
- Overall normalization uncertainty evaluated to 4% including selection criteria and $BR(K^+ \rightarrow \pi^+\pi^0\pi^0)$.

All these sources, being added in quadrature, result in $\sigma_{\text{sys}} = 0.27 \times 10^{-6} \approx 7.5\%$. So the overall error is driven by limited statistics.

Conclusions

The OKA data are analyzed in search for $K^+ \rightarrow \pi^+\pi^0\pi^0\gamma$ decay. The major background source, the decay $K^+ \rightarrow \pi^+\pi^0\pi^0$, is ≈ 5000 times more intense than the radiative decay in question. The RBFN neural network is employed to suppress the background down to Signal:Noise $\approx 1 : 1$ level; about 60 events of the decay observed. The branching ratio obtained by normalization to the decay of similar topology $K^+ \rightarrow \pi^+\pi^0\pi^0$, $BR(K^+ \rightarrow \pi^+\pi^0\pi^0\gamma) = (3.7 \pm 0.9(\text{stat}) \pm 0.3(\text{syst})) \times 10^{-6} (E_\gamma^* > 10 \text{ MeV})$ agrees with ChPT prediction of 3.76×10^{-6} . The γ energy spectrum and angular distribution are also in agreement with ChPT although the errors are large. The observation of the decay proves feasibility of its detailed study on a larger statistical sample.

Acknowledgements We express our gratitude to our colleagues in the accelerator department for the good performance of the U-70 during data taking; to colleagues from the beam department for the stable operation of the 21K beam line, including RF-deflectors, and to colleagues from the engineering physics department for the operation of the cryogenic system of the RF-deflectors. This work was supported by the RSCF Grant N^o22-12-0051.

Data Availability Statement This manuscript has no associated data or the data will not be deposited. The final results obtained during this study are included in this published article. There are no external data associated with the manuscript.

Code Availability Statement The manuscript has no associated code/software. [Author's comment: The code/software generated during the current study could be available from the corresponding author upon reasonable request and collaboration approval.]

Open Access This article is licensed under a Creative Commons Attribution 4.0 International License, which permits use, sharing, adaptation,

distribution and reproduction in any medium or format, as long as you give appropriate credit to the original author(s) and the source, provide a link to the Creative Commons licence, and indicate if changes were made. The images or other third party material in this article are included in the article's Creative Commons licence, unless indicated otherwise in a credit line to the material. If material is not included in the article's Creative Commons licence and your intended use is not permitted by statutory regulation or exceeds the permitted use, you will need to obtain permission directly from the copyright holder. To view a copy of this licence, visit <http://creativecommons.org/licenses/by/4.0/>.
Funded by SCOAP³.

References

1. D'Ambrosio et al., *Z. Phys. C* **76**, 301–310 (1997)
2. V.N. Bolotov et al., *Pisma Zh. Exp. Theor. Fiz* **42**, 390–392 (1985)
3. M.M. Shapkin et al., *Eur. Phys. J. C* **79**(4), 296 (2019)
4. J. Bijnens, F. Borg, *EPJ C* **40**, 383–394 (2005)
5. B. Powell et al., *Nucl. Instrum. Methods* **198**, 217 (1982)
6. F.G. Binon et al., *Nucl. Instrum. Methods A* **248**, 86–102 (1986)
7. V. Kurshetsov et al., *PoS KAON09* **051** (2009)
8. A.S. Sadovsky et al., *Eur. Phys. J. C* **78**, 92 (2018)
9. R. Brun et al., CERN Program Library; W5013 (1993). <https://doi.org/10.17181/CERN.MUHF.DMJ1>
10. R.L. Workman et al. (Particle Data Group), *Prog. Theor. Exp. Phys.* **2022**(8), 083C01 (2022)
11. Schwenker et al., *Neural Netw.* **14**(4:5), 439–458 (2001)
12. V.I. Kravtsov et al., *Eur. Phys. J. C* **79**(7), 635 (2019)